



IJRASET

International Journal For Research in
Applied Science and Engineering Technology



INTERNATIONAL JOURNAL FOR RESEARCH

IN APPLIED SCIENCE & ENGINEERING TECHNOLOGY

Volume: 12 **Issue:** VIII **Month of publication:** August 2024

DOI: <https://doi.org/10.22214/ijraset.2024.63895>

www.ijraset.com

Call:  08813907089

E-mail ID: ijraset@gmail.com

Study of Fluid Flow and Heat Transfer in Microchannel Heat Sinks for Electronics Cooling Application

Kasukurthi Vardhan¹, C. Naga Bhaskar², S Venkateswara Rao³

¹PG Student, ²Professor, ³Assistant Professor, Department of Mechanical Engineering, NRI Institute of Technology, Agiripalli, Vijayawada, A.P

Abstract: Today's age of rapid technological advancements has led to a significant rise in the demand for high-performance electronic chips with high power density. Effective thermal management of such high-power density systems is crucial for their performance, life and reliability. Growing trends of miniaturization and densely packed circuits have necessitated the development of optimized cooling methods, particularly for high-density electronic chips and flexible microelectronic devices. Amongst the presently available cooling techniques such as passive air cooling, forced air cooling, microchannel heat sink, liquid cold plates cooling and heat pipe, the microchannel heat sink technique stands out from the rest owing to its high rate of heat dissipation due to larger surface area to volume ratio. Current work explored three new enhancements in micro channel heat sink (MCHS) for electronic cooling. The new design have different geometry and different enhancement techniques compared with respect to the enhancement over their respective conventional domain. Three dimensional computational models based on finite volume approach were created incorporating the enhancement techniques and analysed numerically in ANSYS Workbench.

Keywords: CFD Analysis, Microchannel, Electronics Cooling

I. INTRODUCTION

Electronic components are getting smaller and smaller, due to which heat generated per unit area is getting bigger. For example, the computers have moved from desktop to wrist watch. In 1970 only a few thousand transistors were placed in a chip, by 2006, one billion were fitted and in 2019, 60 billion transistors are packed in a chip. This results in generation of huge amount of heat in a small space. More than 70% of failure in electronic components is due to thermal mismanagement. Efficient removal of the heat is the major challenge faced by the electronics industry.

Electronics is now a multi trillion-dollar industry having a growth rate of 5 to 8%. Electronics has influenced the day to day activities of all human beings. Automotive, consumer electronics, computers, communication, medical, military are some of the applications of electronics. Electronic packaging is an art of providing a suitable environment to the electronic products for continuous reliable performance. Ergonomics, manufacturing, maintenance, thermal management, shock and vibration are some of the mechanical design aspects to be considered in electronics packaging. Since millions of circuits are placed in a small space, generation of large amount of heat (100 W/cm^2 to more than 200 W/cm^2) takes place. A suitable mechanism to remove this heat is required for prolonged life and reliability of electronic components.

Fan assisted air cooling for electronic components were prominent earlier but have reached the limit of cooling capacity. Water cooled (single phase) microchannel heat sink (MCHS) is one of the promising methods of thermal management of electronic component. Microchannel heat sink is a set of parallel channels having hydraulic diameter between 100 to 1000 microns, length of 5 mm to 35 mm and is fabricated directly on silicon wafer or on copper or aluminium block. Compact size, high surface to volume ratio, low coolant inventory, ability to be mounted on chip to form monolithic configuration are some of the important features of microchannel heat sink. Microchannels with rectangular shape and running parallel to each other are the conventional MCHS used by earlier researchers for heat removal from small spaces.

MCHS is described by overall dimensions such as length (L), breadth (W) and height (H) while the dimensions of a single channel are length (L_c), width (W_c) and depth (H_c) as shown in figure 1.1. The width of wall (W_w) separating the neighbouring channels is also an important dimension and is usually equals to channel width (W_c).

Silicon, copper or aluminium is commonly used material for MCHS. Water, Nitrogen, phase change materials and nano fluids are used as coolants. Water (Single phase and two phase) has been used by majority of researchers. Tuckerman and Pease [1] were the first researchers to use microchannels in electronic cooling in 1981. They etched microchannels 50 μm wide and 300 μm deep on the back side of silicon wafer. Using de-ionised water as coolant they were able to dissipate heat and attain thermal resistance of 0.09 $^{\circ}\text{C}/\text{W}$ over 1 cm^2 area. Since then, huge amount of work is done in the development of microchannel heat sink for electronic cooling. Microchannels of various shape, size and materials have been designed and tested by researchers.

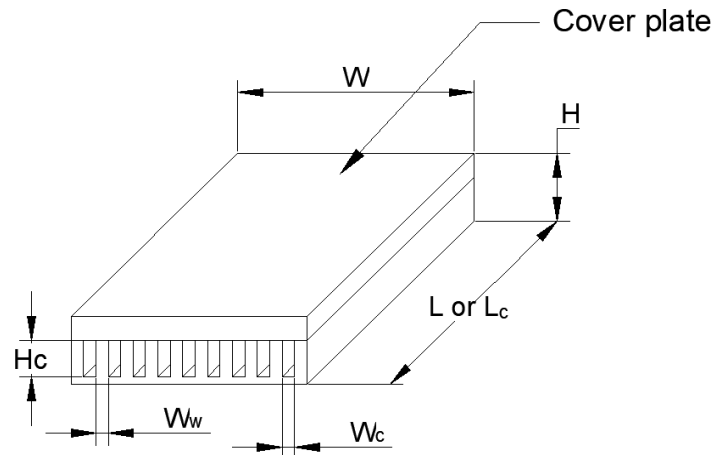


Figure 1.1 Microchannel heat sink showing channel and overall dimensions

The maximum overall dimensions of conventional microchannel heat sink reported by researchers are 35mm x 35mm, while the average overall dimensions are 20mm x 20mm. The single phase, liquid cooled microchannel heat sink mostly has laminar flow type due to the short length scale of channel. If we consider a single microchannel, the velocity of the liquid near wall is zero and maximum at the centre of the channel creating a parabolic velocity profile; in thermal boundary layer the liquid near the wall surface gets heated while the one in the core region is unaffected by the heat. More heat transfer takes place at the entrance region due to thermo-hydraulic entrance effects, and the heat transfer reduces along the channel length resulting in thickening of boundary layer, sensible heat gain by the liquid and rise in temperature along the length of microchannel. Due to the shorter channel length, the liquid passes quickly through the channel and the core part of liquid is unable to remove heat generated at the channel base region. Near the outlet region, high temperature gradient is present between wall surface and liquid in channel core which indicates less heat absorbed by the liquid. This is due to the thick boundary layer which is a major roadblock for the attainment of higher thermal efficiencies in microchannel. Thus, there are some issues with conventional microchannel heat sink which if sorted can improve its performance. A need is felt to have a mechanism to break the thick boundary layer and mix the liquid at different temperatures within the channel which leads to more heat removal from channel walls. Fundamentally, too, for better performance, it is better to have the flow in continuously developing state than a fully developed one in a channel.

Philips [3] extended the theoretical analysis of Tuckerman and Pease [1] to channels having small to large aspect ratios, for developing and fully developed flows, smooth and roughened channel surface. Variable property effects are included for the chip material and coolant. Thermal spreading at the periphery of simulated integrated heat source is also accounted for using simplified one-dimensional models. The numerical analysis results clearly showed that the same thermal performance can be obtained by increasing the channel width from that suggested by analytical results of Tuckerman and Pease [1]. Increasing the channel width causes the flow to become less fully developed at the channel exit. The larger widths help in keeping pumping power requirements below 10 W and are also easier to fabricate. For a heat source of 0.25 cm^2 square heat source, the indium phosphide microchannel heat sink has been tested to a pressure drop of 414 kPa and a thermal resistance as low as 0.072 $^{\circ}\text{C}/(\text{W}/\text{cm}^2)$.

Perret et al. [4] modeled and optimized microchannel design using silicon technology. Microchannels are fabricated using bulk micro-machining on backside of silicon wafer. Another wafer with inlet outlet nozzles and microchannel is fabricated and both wafers are joined by direct bonding technique. The configuration reduces the cooler overall dimensions, reduces the thermal resistance and is compatible with integrated circuits fabrication process. The heat sink dissipated heat flux of 100 W/cm^2 with an increase in junction temperature by 60 $^{\circ}\text{C}$.

Qu and Mudawar [5] investigated numerically and experimentally the pressure drop and heat transfer characteristics of single phase water cooled microchannel heat sink. Rectangular microchannel having a width of 231 μm and height of 713 μm were fabricated on copper block with polycarbonate plastic cover plate. The microchannel was subjected to two heat flux levels of 100 W/cm^2 and 200 W/cm^2 and cooled by de-ionized water having Reynolds number from 139 to 1672. Numerical analysis was done by solving the conjugate heat transfer problem which involved the simultaneous determination of temperature field in both liquid and solid regions. They concluded that both experimental pressure drop and temperature data is in excellent agreement with numerical predictions.

II. NUMERICAL ANALYSIS OF MICROCHANNEL

Microchannels with rectangular shape and running parallel to each other are termed as the conventional MCHS. To improve the thermo-hydraulic performance of conventional MCHS, new enhancements are proposed. Three new MCHS designs viz. enhanced LV- MCHS, enhanced PF-MCHS and enhanced LP-MCHS which employ flow disturbance methods such as secondary channels and flow disturbing pins are described first and then analysed numerically.

A. Enhanced LV-MCHS

The enhanced LV-MCHS is based on leaf venation network that exist in nature. Leaf venation is branching of veins that spread across the leaf to provide structural support and transport of water, minerals and food energy from and to the plant. Different venation patterns are formed due to the presence of various orders of veins. In pinnate type leaf venation (figure 2.1), the primary (1st degree) and secondary (2nd degree) form the major structural veins of the leaf, while the tertiary (3rd degree) and higher order veins though of smaller size, cover the major portion of the leaf. Sample leaves of pinnate type venation were observed under Zeiss microscope (figure 3.2) and its dimensions noted. After studying the dimensions of various pinnate type leaves, the enhanced MCHS with leaf venation pattern is designed.

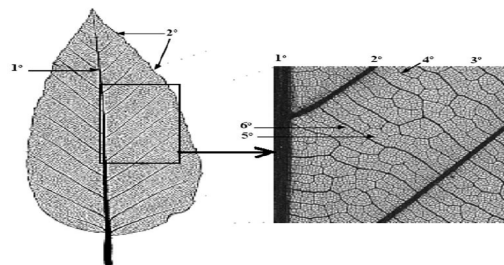


Figure 2.1 Pinnate type leaf venation patterns

So the present work aims at exploring ways to increase flow through secondary channels with minimum pressure drop. The first design in the present work consists of a set made up of three parallel microchannels connected together by alternating secondary channels to create a leaf venation pattern. The set consists of three inlets and two outlets with the central channel outlet closed (figure 3.3 and 3.4). The geometry of microchannel of first design of present work henceforth termed as enhanced LV-MCHS was designed with channel dimensions similar to Lee et al. but having fluid region similar to pinnate leaf venation type.

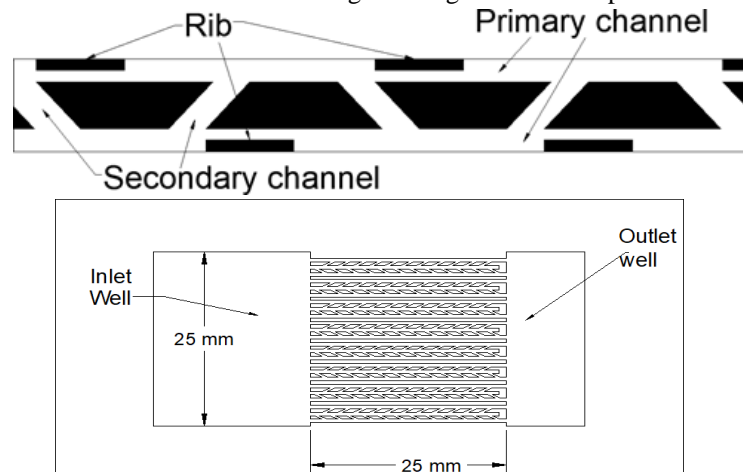


Figure 2.2 Top view of enhanced LV-MCHS

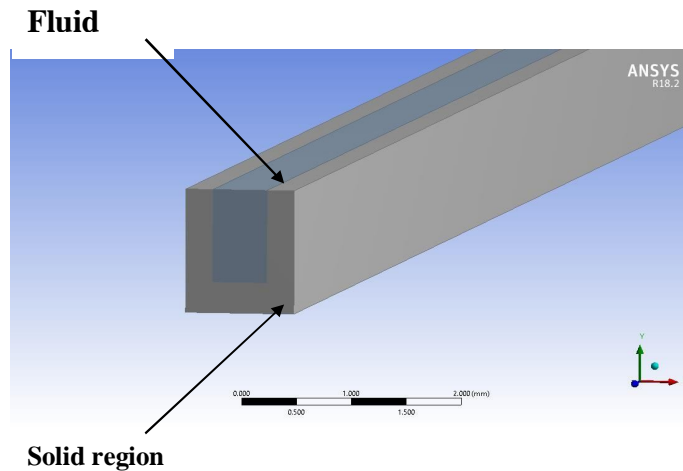
The dimensions of the conventional MCHS and enhanced LV-MCHS are given in table 2.1.

Table 2.1. Dimensions of enhanced LV-MCHS

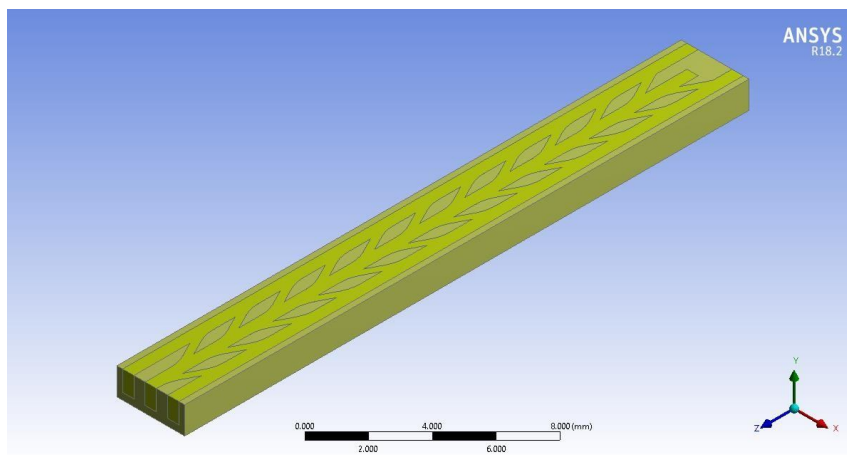
Characteristics	Conventional MCHS	Enhanced LV-MCHS
Material	Copper	Copper
Footprint L x W (mm)	25 x 25	25 x 25
Primary channel width W_c (μm)	500	500
Wall width W_w (μm)	500	500
Channel height H_c (μm)	900	900
Aspect ratio (H_c / W_c)	1.8	1.8
Number of fin rows	24	24
Secondary channel width W_s (μm)	--	300
Secondary channel angle (deg)	--	27

B. Numerical analysis of LV-MCHS

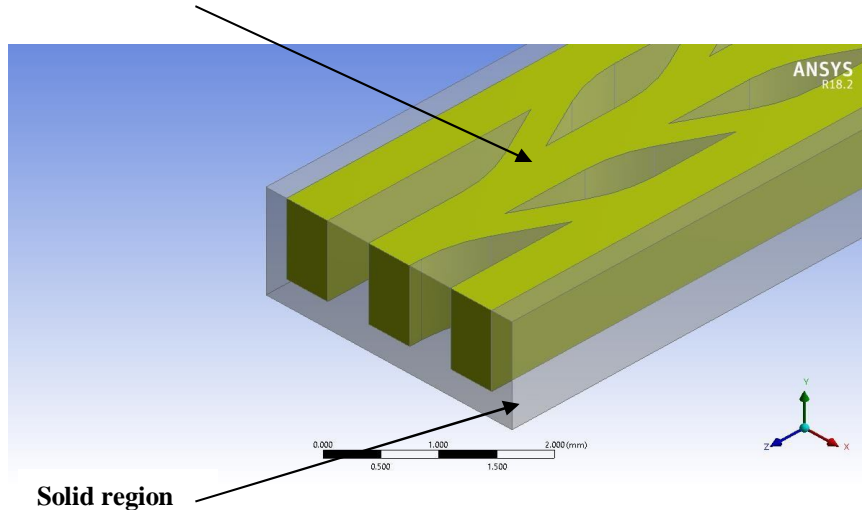
Any engineering problem can be solved using analytical method, experimental method or numerical method. Analytical methods for heat transfer and fluid flow problems are difficult to achieve due to a) the three dimensional equations b) the equations are strongly coupled and non-linear and c) the solution domains are mostly complex. Numerical method holds certain advantages over other methods due to the developments in the computing capabilities and computer codes for complex domains and boundary conditions.



(a)



Fluid region



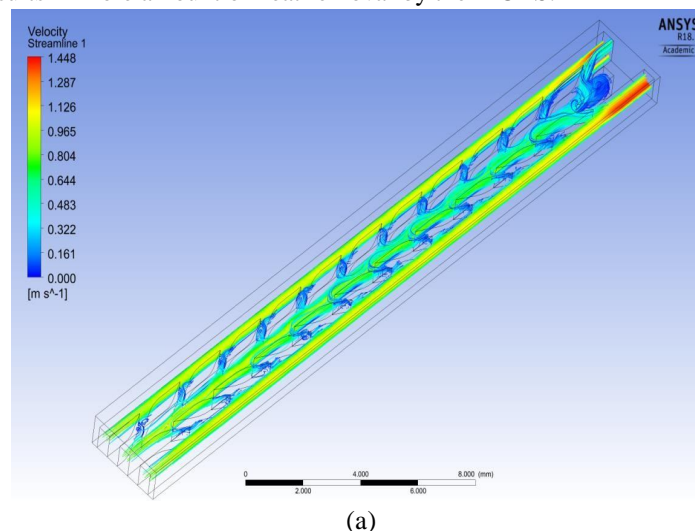
Solid region

Figure 2.3 Computational domain of (a) conventional MCHS (b) enhanced LV-MCHS (c) Close view of LV-MCHS

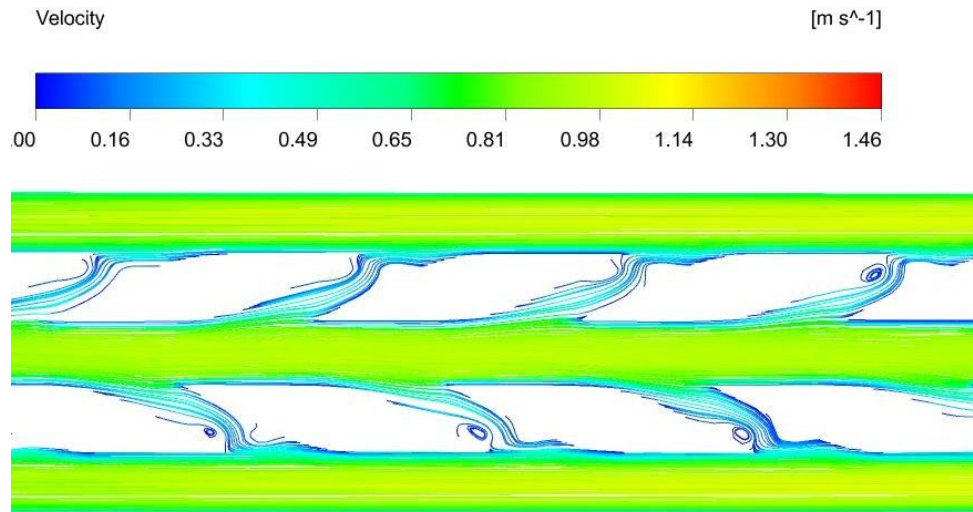
III. RESULTS AND DISCUSSIONS

A. Fluid Flow and Heat Transfer Characteristics

Figure 3.1 (a) shows the three dimensional model with velocity streamlines plotted at the midplane, while the figure 4.1 (b) shows the top view of the velocity streamlines for the central portion of the enhanced LV-MCHS subjected to heat flux of 200 W/cm^2 and flow rate corresponding to Reynolds number of 652. Figure 3.2 shows the velocity streamlines for conventional MCHS for the same region and subjected to same heat flux and flow rate. A fixed flow pattern is visible in conventional MCHS as the streamlines follow a nearly straight path, while a varying pattern is observed in enhanced LV-MCHS. The streamlines in enhanced MCHS near the primary channel walls are interrupted by the inlet of secondary channels as some amount of fluid flows into the secondary channels. The streamlines again become continuous after the inlet region only to be disturbed again by the next secondary channel. The array of secondary channels on either side of central primary channel causes some part of the flow to be diverted into the adjacent primary channel via these secondary channels. This results in the flow in all three primary channels to be constantly in a developing state. The streamlines in the secondary channels indicate that the flow passes smoothly through the secondary channel but meets resistance at the exit from the primary flow flowing in the adjacent primary channel. This causes the flow to change its direction slightly and eventually mix with primary flow. Enhanced MCHS design causes more amount of coolant to come in contact with the surface area. All these factors results in more amount of heat removal by the MCHS.



(a)



(b)

Figure 3.1 Velocity streamlines in primary and secondary channels for (a) 3-d view of the entire enhanced LV-MCHS and (b) top view of central portion of the enhanced LV- MCHS ($q''=200 \text{ W/cm}^2$, $Re=652$)

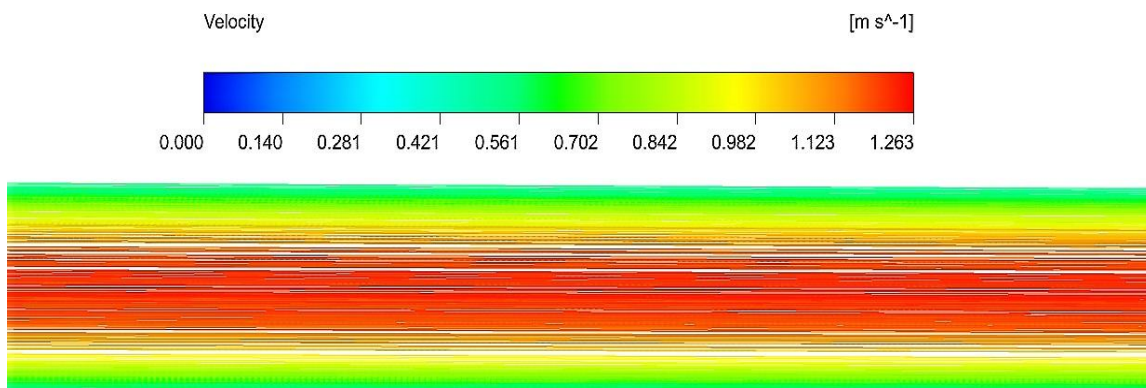
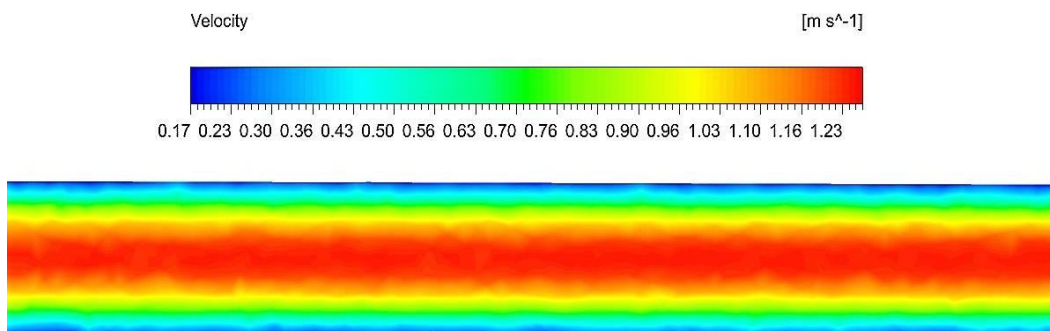


Figure 3.2 Velocity streamlines for conventional MCHS ($q''=200 \text{ W/cm}^2$, $Re=652$)

Velocity distribution in both MCHS is shown in figure 3.3(a) and (b) subjected to heat flux of 200 W/cm^2 , and flow rate corresponding to Reynolds number of 652. In conventional MCHS maximum velocity is concentrated in the central region of the channel and it does not change along the channel length. In enhanced MCHS, the velocity varies along the length as well as across the cross section of the channel. Velocity in the central channel varies from maximum at inlet to zero at the blocked end, while in the neighboring channels it keeps increasing along the length. In enhanced MCHS, the secondary channels have least velocity.



(a)

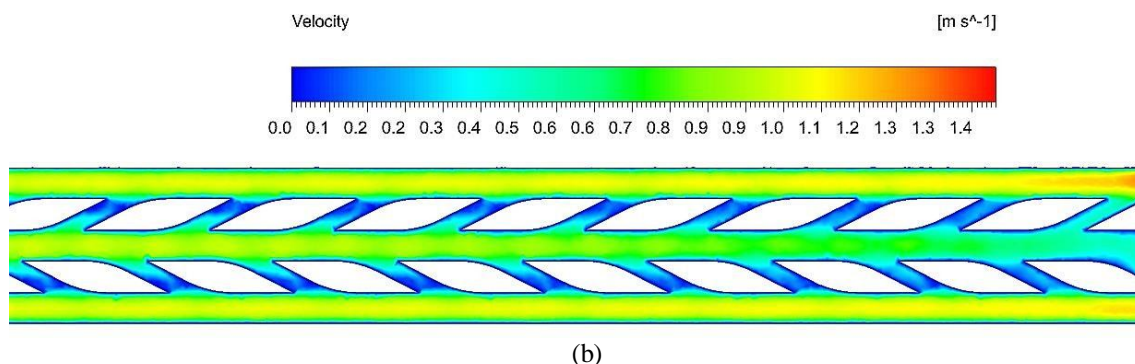


Figure 3.3 Velocity contours for (a) conventional MCHS, (b) enhanced LV-MCHS ($q''=200 \text{ W/cm}^2$, $Re=652$)

B. Performance Analysis

The numerical analysis is performed on both conventional and enhanced LV MCHS for heat flux of 65 to 200 Watt per sq.cm and for each heat flux the Reynolds number corresponding to the flow rate is varied from 652 to 1310. There is appreciable drop in average surface temperature and rise in Nusselt number in the enhanced MCHS design than conventional MCHS indicating enhanced heat transfer due to the new design. But the new design brings additional pressure drop which is two to three times higher than the conventional MCHS.

Performance of conventional and enhanced LV-MCHS is compared for heat flux of 100 Watt per sq.cm. Figure 3.4 shows the effect of Reynolds number on Nusselt number. As expected, for both conventional and enhanced MCHS, there is rise in Nusselt number with increase in Reynolds number. For enhanced MCHS, Nusselt number attained is much higher than for conventional MCHS for both heat flux conditions. The heat removed by enhanced MCHS is two times higher than the conventional MCHS. The rate of increase (slope of the curve) of Nusselt number for both conventional and enhanced MCHS is same. Presence of secondary channels results in additional pressure drop in LV- MCHS as seen in figure 3.5.

Pressure drop increases with increase in Reynolds number for both MCHS, but it increases rapidly for enhanced MCHS at higher flow rates. The pressure drop in enhanced MCHS is nearly three times higher than conventional MCHS. Nusselt number of LV-MCHS is double of Nusselt number in conventional.

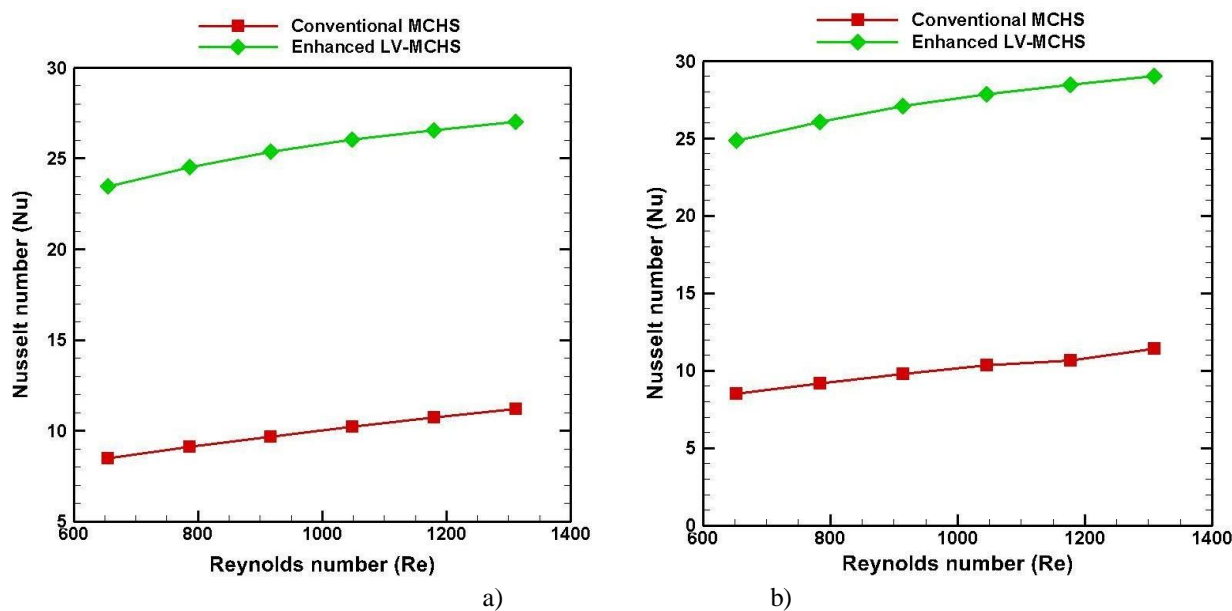


Figure 3.4 Comparison of variation of Nusselt number with Reynolds number for conventional and LV-MCHS for heat flux of a) 100 Watt per sq.cm b) 200 Watt per sq.cm.

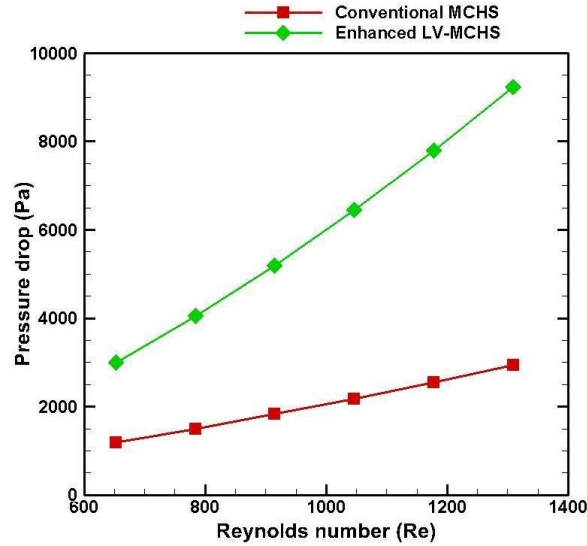


Figure 3.5 Comparison of pressure drop variation of conventional and LV-MCHS with Reynolds number for Heat flux of 100 Watt per sq.cm

The tendency of average bottom surface temperature against Reynolds number for both MCHS is shown in figure 3.6. The average bottom surface temperature decreases with increase in flow rate for both MCHS. The bottom surface temperature indicates the temperature maintained of the component being cooled by the MCHS. The maximum operating temperature of the commercial electronic components is 343K and is 358K for industrial electronics components. The bottom surface temperature for conventional MCHS exceeds the maximum operating temperature for both heat fluxes. Enhanced MCHS bottom surface temperatures are below the maximum limit for a heat flux of 100 Watt per sq.cm, while for heat flux of 200 Watt per sq.cm, the bottom surface temperature is below the limit at higher flow rates only.

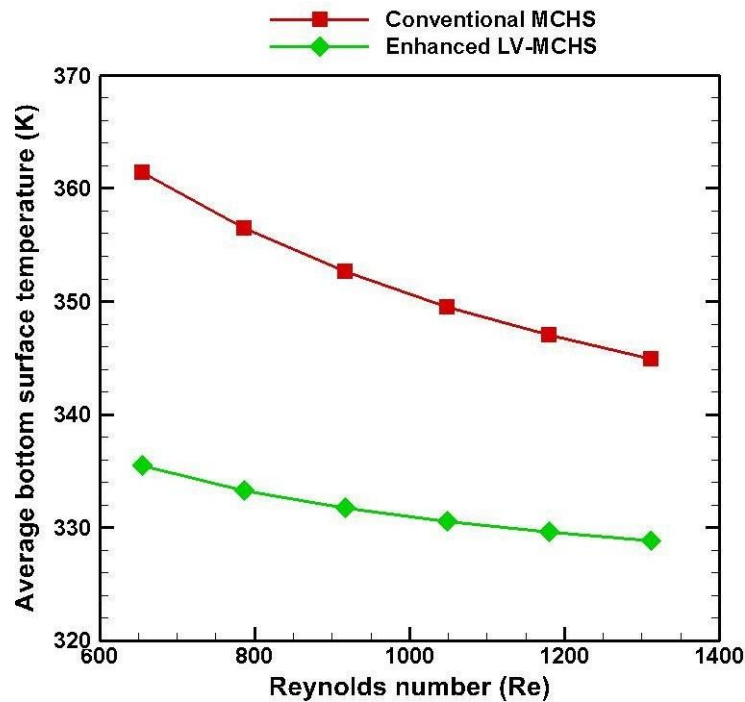


Figure 3.6 Comparison of variation of average bottom surface temperature with Reynolds number of conventional and LV-MCHS for Heat flux of 100 W/cm²

Comparison of various parameters of enhanced MCHS with conventional MCHS is shown in figure 4.11 a) with the subscript 0 indicating the values of conventional MCHS. The Nusselt number ratio decreases with higher Reynolds number. The P/P0 ratio is the pressure drop factor which increases with higher Reynolds number. This is happening due to the condition of less flow through secondary channels at higher flow rates, as the flow does not get sufficient time to divert into secondary channels. Owing to the behavior of above two factors the enhancement factor also decreases with increase in Reynolds number but is more than one which means the overall performance of the enhanced MCHS is superior than conventional MCHS for all flow rates. The performance of current configuration is compared with recent work in extended microchannels (case I) by Yadav et al. (Figure 3.7 b). The enhancement factor is similar at different Reynolds number, the variation is less than 10 percent. The variation can be attributed to the difference in the enhancement design employed in both cases. Figure 3.8 shows the percentage drop in thermal resistance (R/R0) in the enhanced MCHS compared to conventional MCHS for various Reynolds number. The thermal resistance is reduced by a minimum of 50 percent at low Reynolds number and by 55 percent for high Reynolds number.

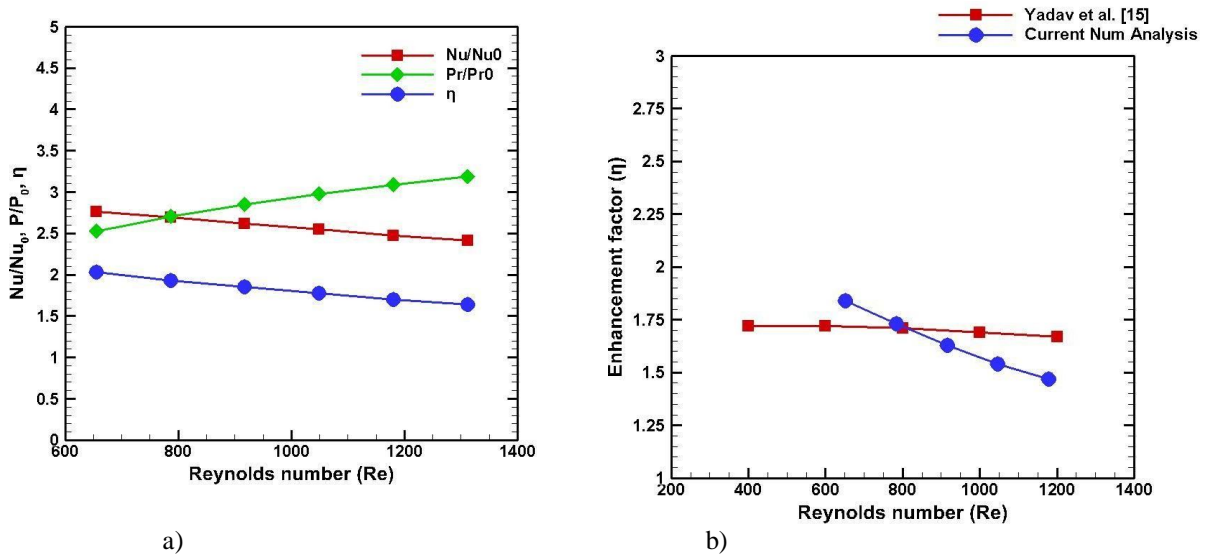


Figure 3.7 Comparison of (a) Variation of pressure, Nusselt number ratios and enhancement factor (η) with Reynolds number ('0' indicates conventional MCHS) of LV-MCHS (b) Comparison of performance of LV-MCHS with Yadav et al. [15] for heat flux of 100 W/cm^2

Conventional electronic components are required to operate over a specified temperature having an upper limit of 343 K for commercial applications and 358 K for industrial applications. Let us consider 353 K as the upper limit for the bottom surface of the MCHS which can be analogous to the electronic components being cooled by MCHS. Figure 3.8 shows the variation of average bottom surface temperature for enhanced MCHS subjected to various heat fluxes at different flow rates

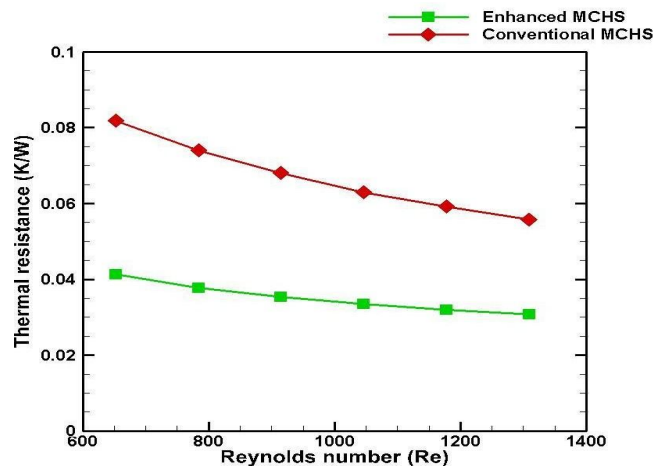


Figure 3.8 Comparison of variation of thermal resistance for different Reynolds number for conventional and LV-MCHS shows more than 80 percent difference

The bottom surface temperature is above the limit only for heat flux of 200 Watt per sq.cm. For the remaining heat fluxes, the bottom surface temperature is below the limit. Thus the enhanced LV- MCHS is suitable for heat flux of 150 Watt per sq.cm and also for heat flux of 200 Watt per sq.cm but using higher flow rates.

IV. CONCLUSIONS

The main aim of this research was to develop new enhancement techniques in conventional MCHS which will increase their heat removing capability. Three dimensional computational models based on finite volume approach were created incorporating the enhancement techniques and analysed numerically in ANSYS WORKBENCH. Each computational model is checked for grid independence during meshing and the numerical results are validated with theoretical results and also with earlier research.

The three designs have different geometry and different enhancement techniques. Hence, they are compared with respect to the enhancement over their respective conventional domain. Comparison of numerical results between three designs shows that the enhanced LV-MCHS has highest enhancement in Nusselt number (Nu/Nu_0) but also has highest pressure drop ratio (Pr/Pr_0). LP-MCHS has the lowest Nu/Nu_0 and lowest Pr/Pr_0 . For a limiting surface temperature of 85°C , LV-MCHS handles the highest heat flux of 200 W/cm^2 .

REFERENCES

- [1] D. B. Tuckerman and R. F. W. Pease, "High-performance heat sinking for {VLSI}," {IEEE} Electron Device Lett., vol. 2, no. 5, pp. 126–129, May 1981.
- [2] M. Steinke and S. Kandlikar, "Review of single-phase heat transfer enhancement techniques for application in microchannels, minichannels and microdevices," Int. J. Heat Technol., vol. 22, pp. 3–11, 2004.
- [3] R. J. Phillips, "Forced-convection, Liquid-cooled, Microchannel Heat Sinks," Mech. Eng., vol. M.S., 1987.
- [4] M. Coyaud, C. Schaeffer, J. Boussey, and C. Perret, "Analytic modeling, optimization, and realization of cooling devices in silicon technology," IEEE Trans. Components Packag. Technol., vol. 23, no. 4, pp. 665–672, 2000.
- [5] W. Qu and I. Mudawar, "Experimental and numerical study of pressure drop and heat transfer in a single-phase micro-channel heat sink," Int. J. Heat Mass Transf., vol. 45, no. 12, pp. 2549–2565, 2002.
- [6] F. Mei, P. R. Parida, J. Jiang, W. J. Meng, and S. V. Ekkad, "Fabrication, assembly, and testing of Cu- and Al-based microchannel heat exchangers," J. Microelectromechanical Syst., vol. 17, no. 4, pp. 869–881, 2008.
- [7] S. G. Kandlikar and W. J. Grande, "Evolution of Microchannel Flow Passages-- Thermohydraulic Performance and Fabrication Technology," Heat Transf. Eng., vol. 24, no. 1, pp. 3–17, 2003.
- [8] P. S. Lee, S. V. Garimella, and D. Liu, "Investigation of heat transfer in rectangular microchannels," Int. J. Heat Mass Transf., vol. 48, no. 9, pp. 1688–1704, 2005.
- [9] S. V. Garimella, V. Singhal, and D. Liu, "On-chip thermal management with microchannel heat sinks and integrated micropumps," Proc. IEEE, vol. 94, no. 8, pp. 1534–1548, 2006.
- [10] W. Qu, I. Mudawar, S.-Y. Lee, and S. T. Wereley, "Experimental and Computational Investigation of Flow Development and Pressure Drop in a Rectangular Micro-channel," J. Electron. Packag., vol. 128, no. 1, p. 1, 2006.
- [11] A. Koşar, "Effect of substrate thickness and material on heat transfer in microchannel heat sinks," Int. J. Therm. Sci., vol. 49, no. 4, pp. 635–642, 2010.
- [12] A. Husain and K.-Y. Kim, "Thermal Optimization of a Microchannel Heat Sink With Trapezoidal Cross Section," J. Electron. Packag., vol. 131, no. 2, p. 21005, 2009.
- [13] S. G. Kandlikar et al., "Heat Transfer in Microchannels{ \textemdash}2012 Status and Research Needs," J. Heat Transfer, vol. 135, no. 9, p. 91001, Jul. 2013.
- [14] V. Yadav, K. Baghel, R. Kumar, and S. T. Kadam, "Numerical investigation of heat transfer in extended surface microchannels," Int. J. Heat Mass Transf., vol. 93, pp. 612– 622, Feb. 2016.
- [15] A. Kosar and Y. Peles, "Thermal-Hydraulic Performance of {MEMS}-based Pin Fin Heat Sink," J. Heat Transfer, vol. 128, no. 2, p. 121, 2006.
- [16] E. G. Colgan et al., "A Practical Implementation of Silicon Microchannel Coolers for High Power Chips," {IEEE} Trans. Components Packag. Technol., vol. 30, no. 2, pp. 218–225, Jun. 2007.
- [17] F. Hong and P. Cheng, "Three dimensional numerical analyses and optimization of offset strip-fin microchannel heat sinks," Int. Commun. Heat Mass Transf., vol. 36, no. 7, pp. 651–656, Aug. 2009.
- [18] H. Shafeie, O. Abouali, K. Jafarpur, and G. Ahmadi, "Numerical study of heat transfer performance of single-phase heat sinks with micro pin-fin structures," Appl. Therm. Eng., vol. 58, no. 1–2, pp. 68–76, Sep. 2013.
- [19] Y. Jia, G. Xia, Y. Li, D. Ma, and B. Cai, "Heat transfer and fluid flow characteristics of combined microchannel with cone-shaped micro pin fins," Int. Commun. Heat Mass Transf., vol. 92, pp. 78–89, Mar. 2018.
- [20] O. O. Adewumi, T. Bello-Ochende, and J. P. Meyer, "Constructal design of combined microchannel and micro pin fins for electronic cooling," Int. J. Heat Mass Transf., vol. 66, pp. 315–323, Nov. 2013.



10.22214/IJRASET



45.98



IMPACT FACTOR:
7.129



IMPACT FACTOR:
7.429



INTERNATIONAL JOURNAL FOR RESEARCH

IN APPLIED SCIENCE & ENGINEERING TECHNOLOGY

Call : 08813907089  (24*7 Support on Whatsapp)